
Volume 14, Issue 4, 142444 (1-14)

Iranian Journal of Catalysis (IJC)

https://doi.org/10.57647/j.ijc.2024.1404.44

# Synthesis and characterization of novel heavy metal (Pd (II), Pt (IV), Au (III)) complexes in the oxidation of benzylic alcohols: investigation of cytotoxicity of them using breast cancer cell line

Jihan Hameed Abdulameer*, Shaymaa Hamzah Daylee, Nada Habeeb Obaid

*Department of Chemistry, College of Education for Pure Sciences, University of Karbala, Iraq.*

***Corresponding author:** jihan.hameed@uokerbala.edu.iq

**Original Research**

Received:
21 June 2024
Revised:
30 September 2024
Accepted:
16 October 2024
Published online:
22 October 2024



**Abstract:**

In this study, a novel amide ligand was synthesized through the two steps. I) Ethyl 4-nitrobenzoate was synthesized through a condensation reaction between p-nitrobenzoic acid and ethanol in the presence of concentrated $H_2SO_4$. II) This compound was further transformed into N, N'-(1,2-phenylene)bis(4-nitrobenzamide) through a chemical reaction with 1, 2-benzene diamine. Novel chelating amide ligands were created using amide and its complexes with metal ions such as Pd (II), Pt (IV), and Au (III). The structures of the new compounds were thoroughly analyzed in the solid state using spectroscopy methods such as $^1$H NMR, UV-Vis, FT-IR, metals and elemental analyses, magnetic sensitivity, and conductance tests at room temperature. The geometry of the resulting complexes was determined to be octahedral for the (Pt-L) complex and square planar for the (Pd-L and Au-L) complexes. The ligand was identified to act as a tetradentate chelate through ($N_2O_2$). The Pd catalyst proved to be effective in the selective oxidation of benzylic alcohols to aldehydes when used alongside pyridine and oxygen gas. The reactions primarily produced aldehydes, with minimal conversion to carboxylic acids through further oxidation. Utilizing low catalyst loadings of 1.6 mol% resulted in high conversion rates of up to 100% and remarkable selectivity of up to 97% for the carbonyl derivatives. The Pd-complex catalyst demonstrated effective catalytic activity and maintained its performance over five cycles without any significant loss in activity, suggesting potential economic benefits. Moreover, an in vitro toxicity bioassay was conducted to evaluate the toxicity of the newly synthesized compounds against MDA cell lines, showing promising results as potential novel anticancer candidates, especially in larger quantities.

**Keywords:** Alcohol; Cancer; Catalyst; Cytotoxicity; Metal complex; Oxidation

## 1. Introduction

Oxidation processes are widely utilized in industrial applications due to their practicality [1–5]. Nevertheless, they are also recognized as some of the most environmentally harmful and dangerous processes. These reactions often result in a high E-factor, which measures the mass of waste produced per mass unit of product. Additionally, significant quantities of toxic byproducts, such as metal salts, are generated in reactions utilizing stoichiometric Cr (VI) or Mn (VII) derivatives or nitrogen oxides in oxidations conducted with $HNO_3$. The conversion of primary and secondary alcohols into their corresponding carbonyl compounds through oxidation holds significant significance in organic synthesis [6–12]. This is primarily due to the extensive applicability of these resultant products as crucial

precursors and intermediates in the production of numerous drugs [13], vitamins [14, 15], and fragrances [16, 17]. The conversion of alcohols into carbonyl compounds plays a crucial role in the fine chemicals sector [18, 19]. Conventional approaches to alcohol oxidation involve the utilization of stoichiometric quantities of inorganic oxidizing agents (e.g., chromate) or organic oxidants (e.g., DMSO). The utilization of these techniques results in environmental and, consequently, economic issues as a result of the substantial quantities of byproducts generated. However, an alternative approach exists that is more ecologically sustainable. This method involves employing molecular oxygen or hydrogen peroxide alongside a catalyst, with water being the primary co-product [20–24]. Various catalysts, both homogeneous and heterogeneous, have been previously studied for the oxidation of alcohols using molecular oxygen or hydrogen peroxide in a liquid medium [25–29]. Effective catalysts utilizing cobalt [30, 31], copper [32–34], palladium [35–40], ruthenium [41, 42], and tungsten [43, 44] have been documented in the case of homogeneous catalysts. Various catalytic systems capable of oxidizing alcohols have been reported for heterogeneous catalysts. In addition, throughout history, the emphasis of research has predominantly been on the utilization of Pt/C [45] or Pd/C [46–48]catalysts. Nevertheless, an inherent limitation of employing Pd or Pt catalysts in the liquid phase with oxygen as the oxidant is their susceptibility to deactivation caused by over-oxidation and poisoning from byproducts [49]. Gold has recently been shown to act as a catalyst in the oxidation of alcohol in the presence of $O_2$ [50–58].

A comprehensive investigation has been conducted on the crystal structure data of basic amides and metal complexes that incorporate monodentate amide ligands [59–61]. The degree of alkylation of the amide functional group, the type of metal ion in the amide complex, and the manner in which it binds to the metal ion are all factors that influence the reported statistical analysis of structural features. The characteristics of metal-ligand coordination compounds are predominantly influenced by the type of ligands that are attached to the metal ion. The field of coordination chemistry has witnessed a significant increase in research focusing on amide ligands, spanning both non-biological and biological domains.

The study of complexes was conducted in order to determine the quantity of bonding and the energy associated with the breast gene. Amides and their derivatives represent a significant group of compounds within the field of organic chemistry. These substances exhibit intriguing biological characteristics, including analgesic, anti-inflammatory, antituberculous, anticonvulsant, antitumor, antimicrobial, and anti-HIV properties. Amides play a crucial role in drug design, serving as potential ligands for metal complexes, facilitating organocatalysis, and enabling the synthesis of heterocyclic compounds. Transition metal chemistry with amide ligands has attracted attention from coordination and bio-inorganic chemists because of the diverse bonding interactions exhibited with electron-rich and electron-poor metals. Breast cancer (BC) ranks as the second most prevalent cancer globally and is the most commonly diagnosed cancer among women [62–64].

This paper presents a comprehensive investigation into the oxidation of alcohols (benzylic) employing amide ligand chelating Au, Pd, and Pt. To ensure a fair comparison, monometallic Au, Pd, and Pt on amide ligands were utilized following a consistent methodology for anticancer activity.

## 2. Experimental

### Materials and Instruments

The reagents from Fluka, Sigma-Aldrich, and Merck were utilized in their original form: p-nitro benzoic acid, DMSO, methanol, hexane, ethyl acetate, 1, 2-benzene diamine, absolute ethanol, and sulfuric acid, along with $PdCl_2$, $H_2PtCl_6$, and $HAuCl_4.H_2O$ were employed in the experiment. The melting points of the synthesized substances were determined using the Kamp m. p apparatus at the University of Karbala. The Euro EA3000 was utilized by Babylon University for elemental microanalysis. Molar conductivity for complexes at the University of Karbala was tested using the Inluba WTW balance. At the University of Al-Nahrain, the magnetic susceptibility balance was employed to ascertain the magnetic susceptibility of the compounds synthesized. The Varian Spectrometer Operating (Bruker) at 400/300 was utilized to perform the Fourier transform, acquiring 1H-NMR spectra. Dimethyl sulfoxide or chloroform served as the solvent, while TMS was employed as the internal standard. At the Laboratory of Tehran University in Iran, measurements were conducted. The University of Bagdad utilized a Schimadzu spectrophotometer, specifically the FT.IR 8400s model to capture FT.IR spectra. These spectra were subsequently analyzed within the wavenumber range of 400-4000 $cm^{-1}$ using a KBr disc. Additionally, the electronic spectra of the ligand and its metal complexes were obtained in a liquid state using the Shimadzu spectrophotometer's UV-Vis, which covered wavelengths from 190 to 1100 nm.

### Synthesis of Ligand (N, N'-(1,2-phenylene) bis(4-nitrobenzamide))

Please follow the instructions provided to prepare the ligand. The synthesis of ethyl 4-nitrobenzoate involves dissolving 0.152 g (0.0018 mol) of p-nitro benzoic acid in 20 mL of pure ethanol, adding 1 mL of concentrated $H_2SO_4$, and then cooling the mixture to 25 $^oC$ after refluxing for three to five hours. The resulting product is filtered, and the absolute ethanol is used for recrystallization to purify it. 0.1 g (0.001 moles) of 1,2-benzene diamine was introduced to 0.33 g (0.002 moles) of ethyl 4-nitrobenzoate in 25 mL of absolute ethanol. Subsequently, the mixture was subjected to reflux for a duration of three hours. The resulting precipitate was filtered, rinsed with cooled ethanol, and subsequently subjected to another round of crystallization using ethanol.

### Synthesis of Metal complexes

A single mole of the identical metal ($PdCl_2$, $H_2PtCl_6$, $HAuCl_4.H_2O$) was dissolved in 5–10 mL of methanol and then combined with one mole of a ligand solution in 30 mL of methanol to form complexes. The reaction mixture was refluxed and stirred at 60 to 65 $^oC$ for a duration of two

hours. Subsequently, the products were dried, washed with ethanol, and filtered.

### General Procedure for the oxidation of benzylic alcohols using Pd-complex

A typical procedure for the experiment involved combining a Pd-complex (0.05 mmol, 60 mg, 1.6 mol%) and toluene (5 mL) in a 25 mL two-necked flask. To this mixture, pyridine (0.2 mL or 5 mmol) was added, resulting in a transformation from a brown suspension to a yellow-white suspension. Oxygen gas was then introduced into the flask from an $O_2$-balloon at atmospheric pressure, and the mixture was heated to 80 °C for 10 minutes. Following this, alcohol (3 mmol) in toluene (5 mL) was injected using a syringe, and the mixture was stirred for an appropriate duration at 90 °C under oxygen gas. After the reaction, the mixture was filtered through a sinter-glass grade with mesh-4. The solvent was removed under reduced pressure, leaving behind an oily residue. This residue was subjected to column chromatography (using hexane: $Et_2O$/EtOAC as eluents) to obtain the desired product. The products obtained were analyzed using GC/MS, and the GLC yields were determined using bibenzyl as an internal standard.

### Cytotoxic assay of metal complexes

The cytotoxicity of the complexes with their ligand was assessed using the colometric N, N'-(1,2-phenylene) bis(4-nitrobenzamide) method. MDA-231 cell lines from the biotechnology center of Al-Nahrain University were utilized in this study. After exposure to different dosages of chemicals, the cell lines were analyzed 24 hours later. The results of the MTT assay, which involved dosages of 400, 200, 100, 50, and 25 g/mL of ligands and heavy metal complexes, were compared to untreated negative controls in the culture media [65].

### Selected Spectroscopic and physical data

**Benzaldehyde (Compound 2a)**: Colorless liquid, 93%, $^1$H NMR (300 MHz, $CDCl_3$, ppm): 7.2 (doublet, J = 5.6 Hz, 1H), 7.3-7.4 (doublet, J = 5.6 Hz, 1H), 7.8 (doublet, J = 5.6 Hz, 1H), 9.6 (singlet, 1H).

**4-chloro-benzaldehyde (Compound 2b)**: Off-white solid, 90%, m. p. 49-51 °C. $^1$H NMR (300 MHz, $CDCl_3$, ppm): 8.0 (doublet, J = 8.2 Hz, 2H), 8.3 (doublet, J = 8.2 Hz, 1H), 9.7 (singlet, 1H).

**4-nitro-benzaldehyde (Compound 2g):** Yellow solid, 86%, m. p. 105-106 °C. $^1$H NMR (300 MHz, $CDCl_3$, ppm): 8.1 (doublet, J = 8.5 Hz, 2H), 8.4 (doublet, J = 8.4 Hz, 2H), 10.2 (singlet, 1H).

**Acetophenone (Compound 2i):** Colorless liquid, 97%. $^1$H NMR (300 MHz, $CDCl_3$, ppm): 2.4 (singlet, 3H), 6.4-6.6 (multiplet, 3H), 7.7 (doublet, J = 8.0 Hz, 2H).

**Benzophenone (Compound 2k):** White crystalline solid, 89%, m. p. 49-51 °C. 1H NMR (300 MHz, $CDCl_3$, ppm): 7.1-7.3 (multiplet, 10H).

## 3. Results and Discussion

### Synthesis and characterization of metal complexes

The ligand, known as N, N'-(1,2-phenylene) bis(4-nitrobenzamide), was easily synthesized via a two-step process (Scheme 1). Initially, the production of ethyl 4-nitrobenzoate entails the dissolution of p-nitrobenzoic acid in 20 mL of ethanol, followed by the addition of 1 mL of concentrated sulfuric acid. Subsequently, the mixture is cooled to a temperature of 25 °C after undergoing reflux for a duration of three to five hours. Next, 0.1 g of 1,2-benzene diamine was added to 0.33 g of ethyl 4-nitrobenzoate in a 25 mL solution of ethanol (EtOH). Following this, the resulting mixture was refluxed for a period of three hours, resulting in the formation of the desired ligand.

Following the synthesis of the ligand, one equivalent of the same metal ($PdCl_2$, $H_2PtCl_6$, $HAuCl_4.H_2O$) was dissolved in 5–10 mL of $CH_3OH$ and mixed with one equivalent of a ligand solution in 30 mL of $CH_3OH$ to create complexes. The resulting mixture underwent reflux and stirring at 60 to 65 °C for a period of two hours. Afterward, the resulting products were dried, rinsed with ethanol, and filtered (Scheme 2).

Table 1presents a comprehensive summary of the physical characteristics and analytical information pertaining to the microelements of the ligand and their corresponding complexes. The results indicate that these observations were

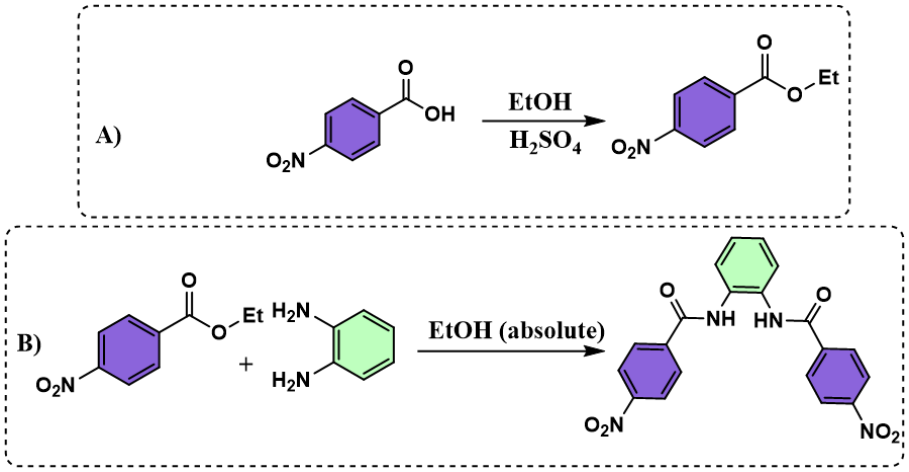


**Scheme 1.** Preparation of amide ligand.

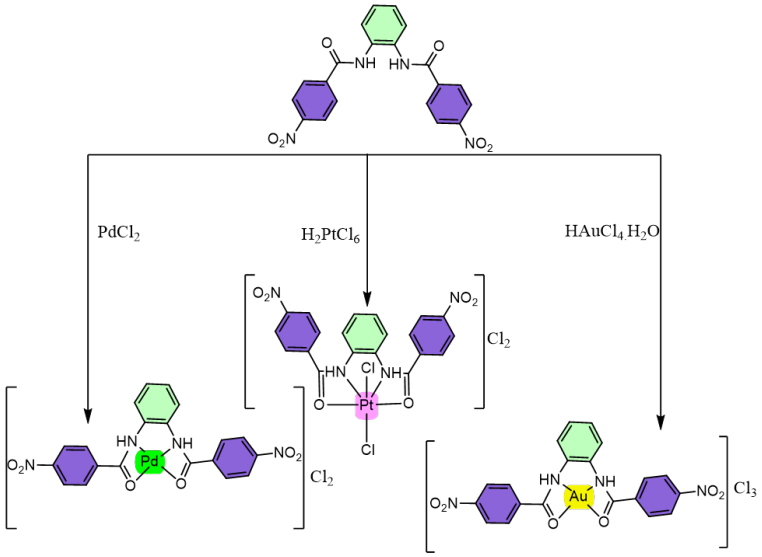


**Scheme 2.** Preparation of metal complex.

not soluble in non-polar or organic solvents but exhibited solubility in dimethyl formamide (DMF) and dimethyl sulfoxide (DMSO), aligning with the anticipated formula. The $^{1}$H-NMR spectra of the platinum complex and the ligand were compared in figures 1and 2 using DMSO-$d_6$ solvent. The free ligand's spectra displayed two signals: one at $\delta$ = 9.351 ppm, corresponding to the amide group's proton, and another at $\delta$= 7.212 - 7.589 ppm, attributed to the protons of the benzene ring. In the complex's spectrum, coordination with the metal ion was evidenced by the chemical shift at 8.526 ppm for the amide group's proton. Infrared spectroscopy research utilizing KBr discs allowed

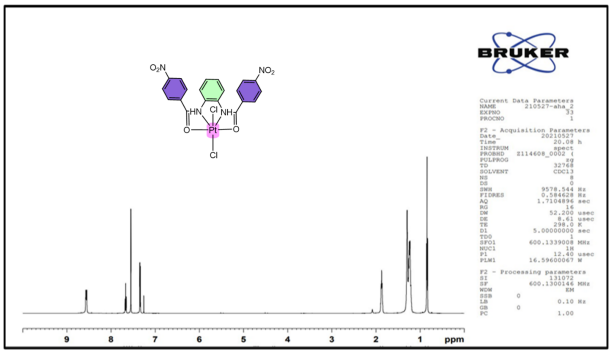


**Figure 1.** $^{1}$H NMR spectrum of ligand

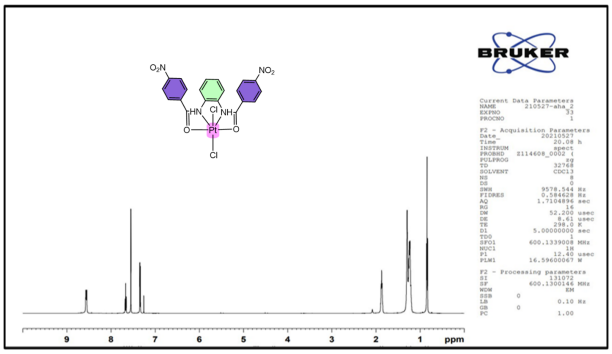


**Figure 2.** $^{1}$H NMR spectrum of Pt-complex

**Table 1.** Physical and analytical data of ligand and metal complex.

| Entry | Com. | Color | M.Wt g/mole | M.P $^{o}$C | Yield% | Found in the elemental analysis (calc.) | | | Metal found% | Proposed Molecular Formula |
|---|---|---|---|---|---|---|---|---|---|---|
| | | | | | | C% | H% | N% | | |
| 1 | L | Yellow | 406.35 | 325-327 | 94.3 | 59.02 (59.12) | 3.31 (3.47) | 13.27 (13.79) | - | $C_{20}H_{14}N_4O_6$ |
| 2 | [Pd-L] | brown | 583.66 | 122-124 | 78 | 47.01 (47.03) | 2.15 (2.37) | 10.19 (10.97) | 20.36 (20.84) | $C_{20}H_{14}Cl_2N_4O_6Pd$ |
| 3 | [Pt-L] | Yellowish orange | 743.22 | 132-134 | 80.1 | 35.23 (35.84) | 1.21 (1.80) | 8.17 (8.36) | 29.01 (29.10) | $C_{20}H_{14}Cl_4N_4O_6Pt$ |
| 4 | [Au-L] | Orange | 710.65 | 163-165 | 89.4 | 39.45 (39.95) | 2.00 (2.01) | 9.18 (9.32) | 32.21 (32.76) | $C_{20}H_{14}AuCl_3N_4O_6$ |

for the recording of solid-state spectra. By comparing the results to existing data, FT-IR analysis offered valuable insights into the coordination of the ligand (L) with various heavy metal ions. The ligand's infrared spectra exhibited a peak at 1629.85 $cm^{-1}$, corresponding to $\upsilon$ (carbonyl), and another peak at 3155.15 $cm^{-1}$ for $\upsilon$ (NH) [66]. The complexes were characterized using FT-IR (figure 3). The confirmation of coordination was supported by the observation of a shift towards higher frequencies for the amide group compared to the free ligand, as well as a shift towards lower frequencies for the carbonyl group. Additional evidence for coordination was provided by the appearance of new bands corresponding to $\upsilon$(M-N) amide at (484-572) $cm^{-1}$ and $\upsilon$(M-O) at (470 $cm^{-1}$) in the spectra of the complexes. The presence of a broad band between (3300 and 2800) $cm^{-1}$ was attributed to moisture in certain samples [67, 68]. Further details regarding the bands observed are outlined in Table 2.

Furthermore, the solubility of the complexes in DMSO, along with data obtained from electronic spectra and magnetic moments, was utilized as a means to confirm the geometry of the produced complexes. UV-Vis spectra of both the ligand and complexes were recorded within the wavelength range of 190 to 1100 nm (refer to figure 4). In the UV-Vis ligand spectra, depicted in Figure 4a, the ($\pi \rightarrow \pi^*$) results in a wide peak observed at 45662-41841 $cm^{-1}$, whereas the ($n \rightarrow \pi^*$) transition exhibits a broad peak at 37735 $cm^{-1}$ [69]. The Brown Pd (II) complex exhibited two bands in its UV-Vis spectra (see figure 4b). The absorption bands corresponding to the spin-paired d8 square planar arrangement were assigned to transitions, with a shoulder initially observed at 29411 $cm^{-1}$ and more intense [70] bands at 36764 $cm^{-1}$. The transitions $^1A_{1g} \rightarrow {}^1B_{1g}$ , with a value of 10 $D_q$, and $^1A_{1g} \rightarrow {}^1E_g$ were also observed in figure 4b [71]. This investigation was conducted based on a comprehensive understanding of square-planar palladium complexes and was compared with existing literature. Further confirmation of square planar stereochemistry was provided by magnetic susceptibility studies, which supported the characterization of the low-spin diamagnetic complex. Conductivity studies indicated that the substance functions as an electrolyte [72, 73].

The electronic spectra of a yellowish-orange platinum (IV) ion complex displayed two absorption bands corresponding to the transitions $^1A_{1g} \rightarrow T_{1g}$ and $^1A_{1g} \rightarrow T_{2g}$ at 27027 and 36363 $cm^{-1}$, respectively (figure 4c). Additionally, a band at 9990 $cm^{-1}$ was observed, indicating spin-prohibited transitions $^1A_{1g} \rightarrow T_{3g}$ and $^3T_{1g}$, as shown in figure 4c. These findings supported the notion of an octahedral geometry for the complex. The magnetic moment of the solid complex was determined to be (0 B.M.), indicating a $t2g^6$ $eg^0$ configuration consistent with spin pair octahedral stereochemistry. The conductance behavior of this complex suggests its electrolytic nature [74].

The gold (III) complex displayed two prominent bands at 23923 and 35842 $cm^{-1}$ in its spectrum. These bands were assigned to the transitions $^1A_{1g} \rightarrow B_{1g}$ and $^1A_{1g} \rightarrow {}^1E_g$, respectively. Another peak band, which appeared diamagnetic with zero magnetic moment (0 B.M.), was believed to be associated with the charge transfer process occurring around the square planar geometry, as depicted in figure 4d. Furthermore, when the electrical conductivity of this compound was measured in DMSO solvent at room temperature, it exhibited ionic activity. Therefore, the spectroscopic methods

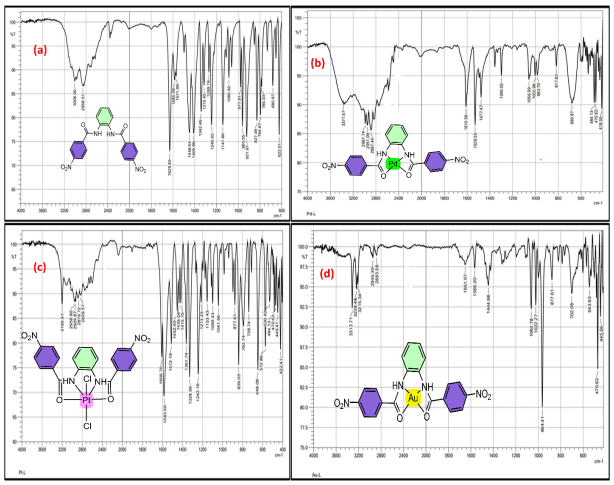


**Figure 3.** FT-IR spectra of a) ligand b) Pd-complex c) Pt-complex d) Au-complex

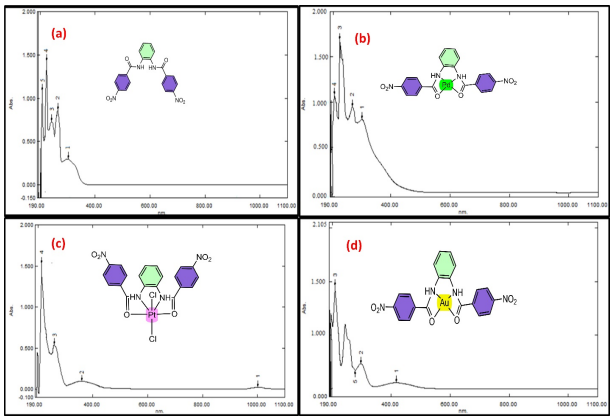


**Figure 4.** UV-Vis spectra of a) ligand b) Pd-complex c) Pt-complex d) Au-complex

**Table 2.** displays the spectrum information of the synthesized compounds.

| Entry | Compound | $\upsilon$ ($NO_2$) | $\upsilon$ (NH) | $\upsilon$ (C=O) | $\upsilon$ (C-H) | $\upsilon$ (M-O) | $\upsilon$ (M-N) |
|---|---|---|---|---|---|---|---|
| 1 | L | 1448.54-1409.96 | 3155.15 | 1629.85 | 3008.95 | - | - |
| 2 | [Pd-L] | 1477.47 | 3371.57 | 1610.65 | 2987.74 | 470.63 | 484.13 |
| 3 | [Pt-L] | 1435.04-1415.75 | 3199.91 | 1606.70 | 2958.80 | 470.63 | 530.42 |
| 4 | [Au-L] | 1444.68 | 3313.17 | 1651.07 | 2945.30 | 470.63 | 543.93 |

**Table 3.** Electronic spectroscopic data, conducting measurements, moments of magnetism in a DMSO solvent, and intricate structural insights.

| Entry | comp. | Abs.cm$^{-1}$ | Assignments | $\mu$eff B.M | $\mu$s.cm$^{-1}$ | Suggested |
|---|---|---|---|---|---|---|
| 1 | L | 37735<br>39062<br>42194 | <br>n $\rightarrow \pi^*$<br>$\pi \rightarrow \pi^*$ | | | |
| 2 | [Pd-L] | 29411<br>36764 | $^1A_{1g} \rightarrow {}^1B_{1g}$<br>$^1A_{1g} \rightarrow {}^1E_g$ | 0.00 | 72.65 | Square planer |
| 3 | [Pt-L] | 27027<br>36363<br>9990 | $^1A_{1g} \rightarrow {}^1T_{1g}$<br>$^1A_{1g} \rightarrow {}^1T_{2g}$<br>$^1A_{1g} \rightarrow {}^3T_{2g}, {}^3T_{1g}$ | 0.00 | 75.77 | Octahedral |
| 4 | [Au-L] | 23923<br>35842<br>44052 | $^1A_{1g} \rightarrow {}^1B_{1g}$<br>$^1A_{1g} \rightarrow {}^1E_g$<br>Au→LCT | 0.00 | 86.62 | Square planer |

and analysis data presented in Table 3 support these findings [75, 76].

### Catalytic evaluation of Pd-complex

To assess the suitability of the Pd-complex, it was utilized for the oxidation of benzylic alcohols, resulting in the formation of corresponding carbonyl compounds. The oxidation of benzyl alcohol to benzaldehyde using a Pd-complex catalyst was first selected as the benchmark reaction for optimizing different reaction conditions, such as catalyst quantity, reaction temperature, base type, oxidant, and solvent (see Table 4). The experimental procedure involved conducting the model reaction with different solvents, including water, ethanol, methanol, toluene, acetonitrile, and benzene, as specified in Table 4 entries 1–6. Toluene was recognized as the most efficient solvent among the choices provided (Table 4, entry 4). Subsequently, the experimental protocol was executed using different reaction temperatures (Table 4, entries 7-9). It is evident that the optimal reaction temperature was 90 °C, and altering the reaction temperature either higher or lower did not have any impact on the yield or duration of the reaction in order to achieve successful results. The experimental procedure involved conducting the model reaction with different bases, specif-

**Table 4.** Optimization of the model reaction.

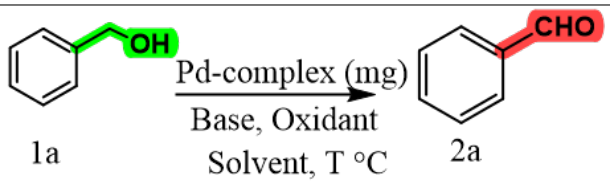


| Entry | Catalyst(mg) | Solvent | T($^o$C) | Base | Oxidant | Time (h) | Yield (%)$^b$ |
|---|---|---|---|---|---|---|---|
| 1 | 60 | $H_2O$ | 90 | Pyridine | $O_2$ | 5 | 25 |
| 2 | 60 | $E_tOH$ | 90 | Pyridine | $O_2$ | 5 | 30 |
| 3 | 60 | MeOH | 90 | Pyridine | $O_2$ | 5 | 25 |
| 4 | 60 | Toluene | 90 | Pyridine | $O_2$ | 2.5 | 93 |
| 5 | 60 | $CH_3CN$ | 90 | Pyridine | $O_2$ | 3.5 | 50 |
| 6 | 60 | Benzene | 90 | Pyridine | $O_2$ | 2.5 | 80 |
| 7 | 60 | Toluene | 70 | Pyridine | $O_2$ | 5 | 80 |
| 8 | 60 | Toluene | 80 | Pyridine | $O_2$ | 3 | 85 |
| 9 | 60 | Toluene | 100 | Pyridine | $O_2$ | 2.5 | 90 |
| 10 | 60 | Toluene | 90 | $Et_3N$ | $O_2$ | 6 | 20 |
| 11 | 60 | Toluene | 90 | $Ph_3P$ | $O_2$ | 5 | 60 |
| 12 | 50 | Toluene | 90 | Pyridine | $O_2$ | 4 | 60 |
| 13 | 70 | Toluene | 90 | Pyridine | $O_2$ | 3 | 85 |
| 14 | 60 | Toluene | 90 | Pyridine | - | 5 | 45 |
| 15 | 60 | Toluene | 90 | Pyridine | $H_2O_2$ | 5 | 80 |
| 16 | No Cat. | Toluene | 90 | Pyridine | $O_2$ | 12 | 15 |
| 17 | No Cat. | Toluene | 90 | Pyridine | $H_2O_2$ | 12 | 10 |
| 18$^c$ | No Cat. | Toluene | 90 | Pyridine | $O_2$ | 24 | 18 |

a) Reaction conditions: alcohol (3.0 mmol), Solvent (5.0 mL), base (5.0 mmol) b), and GC yield. c) In this test, the higher pressure of $O_2$ gas over atmospheric pressure was used (p: 2 bar).

ically triethylamine, pyridine, and triphenylphosphine, as mentioned in Table 4, entries 10-11. Pyridine was identified as the optimal base during our observation. Furthermore, the experimental procedure was conducted in the absence of an oxygen environment, leading to the discovery that oxygen is indeed a necessary component for the reaction to occur (Table 4 entry 14). To demonstrate the effectiveness of the Pd-complex in the oxidation of benzyl alcohol during the model reaction, the experiment was conducted without the presence of the catalyst (Table 4, entries 16-18). The absence of the catalyst results in the yield of the target product not exceeding 15% after 12 hours, even when utilizing various oxidants such as oxygen or hydrogen peroxide. Additionally, to examine the effect of oxygen gas pressure, the model reaction was conducted at an oxygen pressure of 2 bar. Our findings indicate that the yield of benzaldehyde did not surpass 18% after a duration of 24 hours.

The results listed in Table 5 demonstrate the extent of applicability of this enhanced method for oxidizing different benzylic alcohols. Primary benzylic alcohols underwent a transformation to form the corresponding aldehydes with yields ranging from 86% to 96% in a time frame of 2 to 4 hours. This information can be found in Table 5, specifically entries 1 to 8. The experiment illustrated that the existence of electron-donating groups correlates with the enhanced efficiency of the reaction. Secondary benzylic alcohols were readily converted into the corresponding ketones with high efficiency, as evidenced by the high yields obtained (Table 5, entries 9-14). The oxidation of benzoin proceeded at a moderate rate, resulting in the formation of the corresponding diketone with an isolated yield of 83% after 8 hours (refer to Table 5, entry 14).

All experiments were conducted in an oxygen atmosphere due to variations in conversion observed when reactions were performed under argon or nitrogen. This suggests that $O_2$ plays a crucial role in the oxidation process, while palladium complexes remain stable in the absence of $O_2$. A potential mechanism has been outlined to explain these findings (Scheme 3). The mechanistic investigations indicate that initial carbonyl-bound palladium (IV) species form upon reaction with $O_2$, accompanied by the release of pyridine-N-oxide molecules. The catalysts then regenerate, leading to the commencement of a second catalytic cycle.

### The reusability of the catalyst

The study also assessed the reusability and recoverability of the Pd catalyst in the oxidation of 1-phenylethanol to its corresponding product (Table 6). The reused catalyst was collected at the conclusion of each run through straightforward filtration, thoroughly washed with water and ethanol, and then dried at 60 °C. The results confirmed that the Pd catalyst could be reused for five cycles without any notable loss of palladium, as indicated by the ICP data. Interestingly, the amide ligand inhibits the release of Pd ions in any significant quantity.

### Comparison Study

A comparison of the catalytic efficiency of the Pd-amide ligand complex against several documented Pd-based catalysts is shown in Table 7. The findings indicate that the current catalyst shows excellent catalytic activity and significant conversion rates for the oxidation of benzyl alcohol in the presence of oxygen gas, surpassing the results reported in existing literature.

### The cytotoxicity tests

Breast cancer is the most prevalent form of tumor among women worldwide, constituting approximately 25% of all malignant tumors affecting females. Its prevalence extends to various nations, including those that are highly industrialized. Despite the introduction of numerous alternative medications, the response rate to treatment remains disappointingly low. Consequently, there is an urgent imperative to develop more potent anticancer drugs. The majority of research teams are currently dedicated to the creation of an efficacious anticancer drug capable of effectively treating cancer in individuals. This study presents compelling evidence that the synthesized ligand and its complexes exhibit notable anti-breast cancer activity against MDA-MB-231 cell lines. A comprehensive summary of the data, along

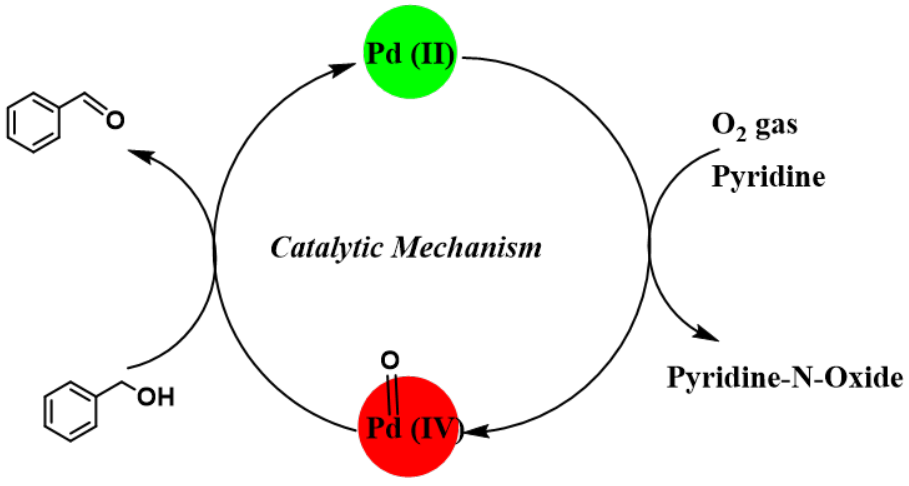


**Scheme 3.** A plausible mechanism for the oxidation of benzyl alcohols to corresponding benzaldehyde catalyzed by Pd (II) complex .

**Table 5.** Pd-complex oxidation of benzylic alcohols[a]

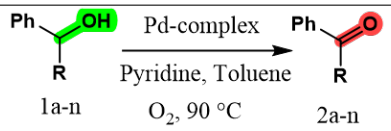


**R: H, $CH_3$, $C_2H_5$, Ph**

| Entry | Starting alcohol | Product | Conv.(%) | Yield (%)[b] | Time (h) | TON | TOF ($h^{-1}$) |
|---|---|---|---|---|---|---|---|
| 1 | 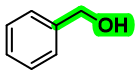 1a | 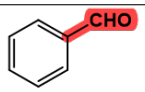 2a | 100 | 93 | 2.5 | 58 | 23.2 |
| 2 | 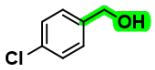 1b | 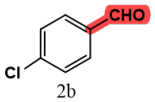 2b | 99 | 90 | 4.0 | 56 | 14.0 |
| 3 | 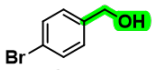 1c | 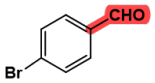 2c | 98 | 91 | 3.5 | 57 | 16.3 |
| 4 | 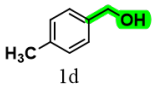 1d | 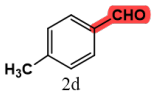 2d | 100 | 95 | 2.5 | 59 | 23.6 |
| 5 | 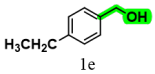 1e | 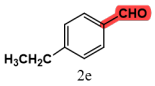 2e | 100 | 94 | 2.5 | 59 | 23.6 |
| 6 | 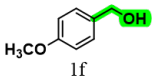 1f | 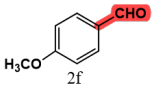 2f | 100 | 96 | 2.0 | 60 | 30.0 |
| 7 | 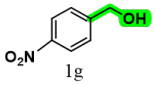 1g | 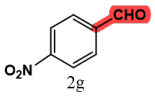 2g | 95 | 86 | 4.0 | 54 | 13.5 |
| 8 | 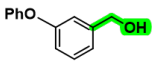 1h | 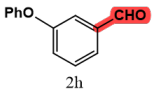 2h | 93 | 88 | 4.0 | 55 | 13.8 |
| 9 | 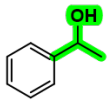 1i | 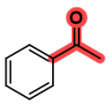 2i | 100 | 97 | 3.0 | 61 | 20.3 |
| 10 | 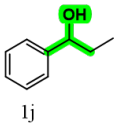 1j | 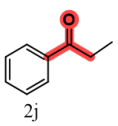 2j | 100 | 92 | 3.5 | 58 | 16.6 |
| 11 | 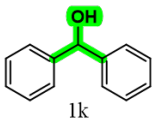 1k | 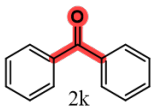 2k | 95 | 89 | 4.5 | 56 | 12.4 |

Continue of Table 5

| Entry | Starting alcohol | Product | Conv.(%) | Yield (%)[b] | Time (h) | TON | TOF ($h^{-1}$) |
|---|---|---|---|---|---|---|---|
| 12 | 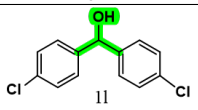 1l | 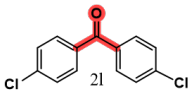 2l | 90 | 86 | 5.0 | 54 | 10.8 |
| 13 | 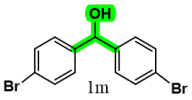 1m | 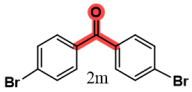 2m | 92 | 88 | 5.5 | 55 | 10.0 |
| 14 | 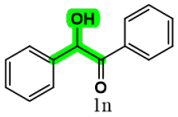 1n | 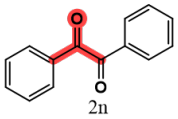 2n | 90 | 83 | 8.0 | 52 | 6.5 |

a)General reaction conditions: starting alcohols (3.0 mmol), Toluene (5.0 mL), Pyridine (5.0 mmol), catalyst: 60 mg (1.6 mol%), T: 90 $^{o}$C, under $O_2$ atmosphere. b) GC yields.

**Table 6.** Screening of the reusability of Pd-complex a

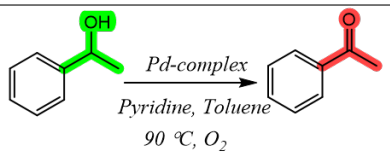


| Run | Conversion (%)[b] | Yield (%)[c] | Pd leaching (%)[d] | Time (h) | TON | TOF ($h^{-1}$) |
|---|---|---|---|---|---|---|
| 1st | 100 | 97 | 0.05% | 3 | 60.6 | 20.2 |
| 2nd | 100 | 96 | 0.04% | 3 | 60.0 | 20.0 |
| 3rd | 98 | 97 | 0.14% | 3.5 | 60.6 | 17.3 |
| 4th | 98 | 95 | 0.68% | 4.0 | 59.4 | 14.8 |
| 5th | 93 | 91 | 1.2% | 4.5 | 56.9 | 12.6 |

a)a) Reaction conditions: 1-Phenylethanol: 3.0 mmol; Toluene: 5.0 mL; Pyridine: 5.0 mmol; T: 90 $^{o}$C; Catalyst: 60 mg; P $O_2$: atmospheric pressure. b) GC yields based on the starting materials, c) GC Yields, d) Palladium leaching based on the ICP .

**Table 7.** A comparison study between the catalytic activity of different Pd based catalysts for the oxidation of benzyl alcohols

| Entry | Catalyst | Reaction conditions | Conv.(%) | Product Selec.(%) | Ref. |
|---|---|---|---|---|---|
| 1 | Pd@U-E15 | $H_2O$, $K_2CO_3$, $O_2$, 90 $^{o}$C | 90 | 90 | [77] |
| 2 | Pd-NaX Zeolite | Toluene, $O_2$, 100 $^{o}$C | 66 | 97 | [78] |
| 3 | Pd-SBA-15 | p-Xylene, $O_2$, 120 $^{o}$C | 99 | 90 | [79] |
| 4 | Pd-Pol | $H_2O$, $K_2CO_3$, Air, 100 $^{o}$C | 98 | >99 | [80] |
| 5 | $Pd/Al_2O_3$ | Solvent free, $O_2$, 120 $^{o}$C | 80 | 94 | [81] |
| 6 | Pd@Cu(II)-MOF | Xylene, air, 130 $^{o}$C | 95 | >99 | [82] |
| 7 | CQDs-TPy/Pd NPs | EtOH/$H_2O$, $K_2CO_3$ air, 90 $^{o}$C | 85 | >99 | [38] |
| 8 | AuPd-PVA/$TiO_2$ | $O_2$, 120 $^{o}$C | 72 | 69 | [83] |
| 9 | Pd/MagSBA | Solvent free, $O_2$, 85 $^{o}$C | 83 | 80 | [84] |
| 10 | Pd/CNTs | Xylene, air, 90 $^{o}$C | 89 | 98 | [**?** ] |
| 11 | Pd/HMSNs Pyra/Pd | EtOH, $H_2O_2$, 60 $^{o}$C | 70 | 99 | [85] |
| 12 | Pd-Amide ligand complex | Toluene, Pyridine, T: 90 $^{o}$C, under $O_2$ atmosphere | 100 | 93 | This work |

with the least significant difference (LSD Value), is provided in Table 8.

Following the treatment, the cells were subjected to incubation with MDA-MB-231 for a complete day. Subsequently, the cells were exposed to different concentrations (25, 50, 100, 200, and 400 g/mL) of newly synthesized compounds. To assess the cytotoxicity and viability of the cells, the MTT test was employed, and the results were documented in Table 8 and figure 5. Comparing the findings to the untreated negative control cells, it was observed that both

**Table 8.** The % inhibition rate on MDA cell lines is displayed

| Entry | Compound | C400% | C200% | C100% | C50% | C25% | LSD value |
|---|---|---|---|---|---|---|---|
| 1 | L | 79 | 65 | 48 | 43 | 40 | 8.93 ** |
| | | A a | A ab | B b | A d | A d | |
| 2 | [Pd-L] | 90 | 79 | 72 | 50 | 33 | 9.01 ** |
| | | A a | A a | B b | A c | B d | |
| 3 | [Pt-L] | 93 | 82 | 75 | 57 | 43 | 8.47 ** |
| | | A a | A a | A a | B b | A b | |
| 4 | [Au-L] | 97 | 88 | 85 | 61 | 48 | 8.52 ** |
| | | A a | A a | B b | A c | A d | |
| 5 | LSD value | 5.04 NS | 4.88 NS | 6.92 ** | 6.71 ** | 7.36 ** | — |

Significant differences exist between means that have distinct capital letters in the same column and small characters in the same row. ** ($P<0.01$).

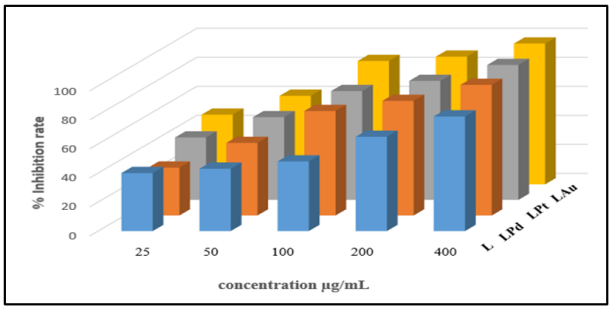


**Figure 5.** The inhibition rate on an MDA cell line as a percentage following a 24-hour exposure to produced compounds.

the free ligands and the metal complexes exhibited significant suppression rates in the MTT experiment. Notably, at high concentrations of 400 g/mL for each of [Pd-L], [Pt-L], and [Au-L], respectively, all metal complexes demonstrated considerable toxicity compared to the ligand, resulting in high inhibition rates of 90, 93, and 97 percent. As the concentrations gradually decreased from high to low, the inhibition rates also decreased. The pharmacological effects of these complexes can be attributed to various factors, including their ability to mimic natural substances and hinder the growth and activity of breast cancer cells through the apoptosis and autophagy pathways.

### Computational study of ligand and metal complexes

Due to the intricate nature of metal complexes, the ligand structures and their corresponding metal complexes were optimized using the 6-31$^{++}$G** and 6-31G$^{++}$ basis sets, respectively (figure 6). Furthermore, Table 9 and figure 6 display the molecular orbitals of both the ligand and its metal complexes (See supporting information data).

## 4. Conclusion

This study highlights the effectiveness of amide ligands in chelating palladium (Pd), platinum (Pt), and gold (Au), leading to the creation of highly efficient catalysts. The structural configurations of the resulting complexes

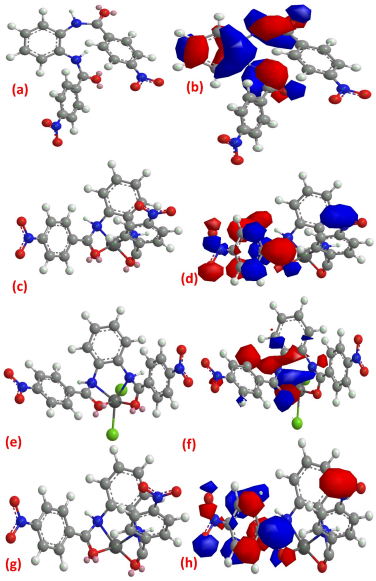


**Figure 6.** Optimization structure using DFT calculation of (a) Ligand (c) Pd-complex (e) Pt-complex (g) Au-complex and molecular orbital (HOMO) of (b) Ligand (d) Pd-complex (f) Pt-complex (h) Au-complex.

**Table 9.** More information for DFT calculation of ligand and Pd, Pt, and Au complexes

| Entry | Stretch | Bend | Stretch-Bend | Torsion | Non-1,4 VDW | 1,4 VDW | Charge /Charge | Charge /Dipole | Dipole /Dipole | Total Energy |
|---|---|---|---|---|---|---|---|---|---|---|
| Ligand | 1.5419 | 18.8215 | 0.2213 | 6.8467 | -2.95 | 18.2514 | 0.0375 | 0.4641 | -13.3535 | 29.8718 kcal/mol |
| Au- | 19.0090 | 1784.5817 | -10.749 | 107.5461 | -4.72 | 19.4584 | 0.1547 | 1.9528 | -4.8176 | 1912.4104 kcal/mol |
| Pd- | 6.1949 | 1725.9631 | -5.3427 | 104.0236 | -4.79 | 20.6603 | 0.1918 | 2.0215 | -4.7709 | 1844.1431 kcal/mol |

were analyzed using advanced techniques, including amide and spectroscopy tests, elemental analysis (AA and CHN), magnetic dipole moment measurements, and complex conductivity assessments at room temperature. The findings suggest that the Pt (IV) complex adopts an octahedral geometry with six coordination sites, while the Pd (II) and Au (III) complexes exhibit square planar structures with four coordination sites in their solid states. The Pd catalyst shows outstanding capabilities in the selective oxidation of benzylic alcohols under oxygen gas pressure, providing benefits such as easy recovery and effective regeneration. Remarkably, the Pd catalyst achieves up to 100% conversion rates and demonstrates excellent selectivity for aldehydes, reaching up to 97%. Additionally, the catalyst maintains favorable activity and stability, as evidenced by successful recycling and reuse over five cycles with minimal performance loss. Given the impressive catalytic properties of the Pd amide complex, it is anticipated to have significant potential for future applications. Our ongoing research is dedicated to further investigating catalytic systems for alcohol oxidation using other metals, including Au and Pt complexes. Furthermore, these compounds were tested against the anticancer MDA cell line, showing that increased compound concentration correlates with enhanced efficacy in killing cancer cells. The synergistic effects of these complexes were found to exert a more pronounced biological impact compared to the free ligand.

**Acknowledgement**
The authors are thankful to the SERB-SURE, GOI (SUR/2022/002631) and RCUB (RCU-IDR-2022-23) for the financial support to Dr. KK.

**Supplementary information**
Catalyst characterization and UV-Vis Profiles are available in supplementary.

**Authors Contributions**
Authors were equally contributed in acquisition and analysing the data as well as preparing the paper.

**Availability of Data and Materials**
Data is available on request from the corresponding author, upon reasonable request.

**Conflict of Interests**
The authors declare that they have no known competing financial interests or personal relationships that could have appeared to influence the work reported in this paper.



## References

[1] T. Mandal, S. Maity, D. Dasgupta, and S. Datta. *Desalination*, **250**(2010):87–94, . DOI: https://doi.org/10.1016/j.desal.2009.04.012.

[2] T. Mandal, D. Dasgupta, S. Mandal, and S. Datta. *J. Hazard. Mater.*, **180**(2010):204–211, . DOI: https://doi.org/10.1016/j.jhazmat.2010.04.014.

[3] G. Hong Tran, T. Khanh Tran, H.-J. Leu, D. Richards, and S.-S. Lo. *Arabian Journal of Chemistry*, **17**(2024):105611. DOI: https://doi.org/10.1016/j.arabjc.2024.105611.

[4] V. Kolkovsky. *physica status solidi (a)*, ():2400281. DOI: https://doi.org/10.1002/pssa.202400281.

[5] S. Abu-Melha. *Polyhedron*, **252**(2024):116781. DOI: https://doi.org/10.1016/j.poly.2023.116781.

[6] N. Nath, S. Chakroborty, K. Pal, A. Barik, N. Priyadarsini Mishra, and S. Kralj. *Top. Catal.*, **67**(2024):192–202. DOI: https://doi.org/10.1007/s11244-023-01839-y.

[7] H. Alamgholiloo, S. Rostamnia, K. Zhang, T. H. Lee, Y.-S. Lee, R. S. Varma, H. W. Jang, and M. Shokouhimehr. *ACS Omega*, **5**(2020):5182–5191. DOI: https://doi.org/10.1021/acsomega.9b04209.

[8] Z. Sun, X. Yang, X. F. Yu, L. Xia, Y. Peng, Z. Li, Y. Zhang, J. Cheng, K. Zhang, and J. Yu. *Applied Catalysis B: Environmental*, **285**(2021):119790. DOI: https://doi.org/10.1016/j.apcatb.2020.119790.

[9] G. Lu, X. Huang, Y. Li, G. Zhao, G. Pang, and G. Wang. *J. Energ. Chem.*, **43**(2020):8–15. DOI: https://doi.org/10.1016/j.jechem.2019.07.014.

[10] A. H. C. Khavar, Z. Khazaee, A. R. Mahjoub, and R. Nejat. *J. Photochem. Photobiol. A: Chem.*, **431**(2022):114020. DOI: https://doi.org/10.1016/j.jphotochem.2022.114020.

[11] P. Chandra, T. Ghosh, N. Choudhary, A. Mohammad, and S. M. Mobin. *Coord. Chem. Rev.*, **411**(2020):213241. DOI: https://doi.org/10.1016/j.ccr.2020.213241.

[12] X. Zhao, Q. Liu, Q. Li, L. Chen, L. Mao, H. Wang, and S. Chen. *Chem. Eng. J.*, **400**(2020):125744, . DOI: https://doi.org/10.1016/j.cej.2020.125744.

[13] Z. X. He, B. Yin, X. H. Li, X. L. Zhou, H. N. Song, J. B. Xu, and F. Gao. *J. Org. Chem.*, **88**(2023):4765–4769. DOI: https://doi.org/10.1021/acs.joc.2c02667.

[14] R. Hong, R. T. Lan, Y. Ren, L. Xu, Y. X. Xu, N. A. Shah, R. M. Gul, S. Huang, L. Li, J. Z. Xu, Z. M. Li, and K. Li. *Polymer*, **295**(2024):126773. DOI: https://doi.org/10.1016/j.polymer.2024.126773.

[15] S. Kundu and D. Sarkar. *J. Heterocycl. Chem.*, **60**(2023):345–368. DOI: https://doi.org/10.1002/jhet.4565.

[16] J. De Maron, T. Tabanelli, F. Ospitali, C. Lopez Cruz, P. Righi, and F. Cavani. *Catal. Sci. Technol.*, **13**(2023):1059–1073. DOI: https://doi.org/10.1039/D2CY01836E.

[17] M. C. Cancellieri, D. Maggioni, L. Di Maio, D. Fiorito, E. Brenna, F. Parmeggiani, and F. G. Gatti. *Green Chem.*, **26**(2024):6150–6159. DOI: https://doi.org/10.1039/D4GC00746H.

[18] R. K. Sharma, R. Bandichhor, V. Mishra, S. Sharma, S. Yadav, S. Mehta, B. Arora, P. Rana, S. Dutta, and K. Solanki. *Materials Advances*, **4**(2023):1795–1830. DOI: https://doi.org/10.1039/D2MA00977C.

[19] D. Tang, G. Lu, Z. Shen, Y. Hu, L. Yao, B. Li, G. Zhao, B. Peng, and X. Huang. *J. Energ. Chem.*, **77**(2023):80–118. DOI: https://doi.org/10.1016/j.jechem.2022.10.038.

[20] U. R. Pillai and E. Sahle–Demessie. *J. Catal.*, **211**(2002):434–444. DOI: https://doi.org/10.1006/jcat.2002.3771.

[21] T. Mallat and A. Baiker. *Catal. Today,*, **19**(1994): 247–283. DOI: https://doi.org/10.1016/0920-5861(94)80187-8.

[22] C. Venturello and M. Gambaro. *J. Org. Chem.*, **56**(1991):5924–5931. DOI: https://doi.org/10.1021/jo00020a040.

[23] K. Sato, M. Aoki, J. Takagi, and R. Noyori. *J. Am. Chem. Soc.*, **119**(1997):12386–12387. DOI: https://doi.org/10.1021/ja973412p.

[24] T. H. Zauche and J. H. Espenson. *Inorg. Chem.*, **37**(1998):6827–6831. DOI: https://doi.org/10.1021/ic9806784.

[25] Z. F. Yuan, W. N. Zhao, Z. P. Liu, and B. Q. Xu. *J. Catal.*, **353**(2017):37–43. DOI: https://doi.org/10.1016/j.jcat.2017.05.006.

[26] W. G. Lloyd. *J. Org. Chem.*, **32**(1967):2816–2819. DOI: https://doi.org/10.1021/jo01284a038.

[27] V. V. Torbina, A. A. Vodyankin, S. Ten, G. V. Mamontov, M. A. Salaev, V. I. Sobolev, and O. V. Vodyankina. *Catalysts*, **8**(2018):447.

[28] L. Chen, J. Tang, L. N. Song, P. Chen, J. He, C. T. Au, and S. F. Yin. *Applied Catalysis B: Environmental*, **242**(2019):379–388, . DOI: https://doi.org/10.1016/j.apcatb.2018.10.025.

[29] J. Jover, M. Garcia-Rates, and N. López. *ACS Catal.*, **6**(2016):4135–4143. DOI: https://doi.org/10.1021/acscatal.6b00832.

[30] M. Li, S. Wu, X. Yang, J. Hu, L. Peng, L. Q. Bai, Huo, and J. Guan. *Appl. Catal., A*, **543**(2017):61–66, . DOI: https://doi.org/10.1016/j.apcata.2017.06.018.

[31] J. Zhu, K. Kailasam, A. Fischer, and A. Thomas. *ACS Catal.*, **1**(2011):342–347. DOI: https://doi.org/10.1021/cs100153a.

[32] D. Ramakrishna and B. R. Bhat. *Inorg. Chem. Commun.*, **14**(2011):690–693. DOI: https://doi.org/10.1016/j.inoche.2011.02.007.

[33] J. U. Ahmad, M. T. Raisanen, M. Leskela, and T. Repo. *Appl. Catal., A*, **411-412**(2012):180–187. DOI: https://doi.org/10.1016/j.apcata.2011.10.038.

[34] P. Gamez, I. W. C. E. Arends, R. A. Sheldon, and J. Reedijk. *Adv. Synth. Catal.*, **346**(2004):805–811. DOI: https://doi.org/10.1002/adsc.200404063.

[35] J. Muzart. *Tetrahedron*, **59**(2003):5789–5816. DOI: https://doi.org/10.1016/S0040-4020(03)00866-4.

[36] Y. Tamaru, Y. Yamada, K. Inoue, Y. Yamamoto, and Z. Yoshida. *J. Org. Chem.*, **48**(1983):1286–1292. DOI: https://doi.org/10.1021/jo00156a028.

[37] G. Xu, L. Dai, M. Du, A. Peng, G. Zeng, H. Chen, R. Yan, and W. Li. *ACS Sustainable Chemistry and Engineering*, **12**(2024):2751–2760, . DOI: https://doi.org/10.1021/acssuschemeng.3c07316.

[38] H. Targhan, A. Rezaei, A. Aliabadi, A. Ramazani, Z. Zhao, and H. Zheng. *Sci. Rep.*, **14**(2024):536. DOI: https://doi.org/10.1038/s41598-023-49526-y.

[39] X. Feng, S. Shi, G. Zhu, Y. Wang, J. Cao, and J. Xu. *ACS Catal.*, **14**(2024):776–784. DOI: https://doi.org/10.1021/acscatal.3c04779.

[40] X. Jiang, Y. Chen, Z. Gao, C. Li, J. Li, and X. Huang. *Inorg. Chem. Commun.*, **159**(2024):111798. DOI: https://doi.org/10.1016/j.inoche.2023.111798.

[41] N. F. Nunheim and W. R. Thiel. *ChemCatChem*, **16**(2024):e202301120. DOI: https://doi.org/10.1002/cctc.202301120.

[42] N. Ganji, B. Karimi, and H. Vali. *ACS Applied Nano Materials*, **7**(2024):2650–2661. DOI: https://doi.org/10.1021/acsanm.3c04780.

[43] M. J. da Silva, P. H. da Silva Andrade, T. A. Silva, M. B. T. Diniz, S. O. Ferreira, R. C. da Silva, and E. N. D. de Araujo. *Catal. Lett.*, **154**(2024): 1648–1663. DOI: https://doi.org/10.1007/s10562-023-04441-9.

[44] C. Xu, R. Zeng, P. K. Shen, and Z. Wei. *Electrochim. Acta*, **51**(2005):1031–1035, . DOI: https://doi.org/10.1016/j.electacta.2005.05.041.

[45] C. Xu, R. Zeng, P. K. Shen, and Z. Wei. *Electrochim. Acta*, **51**(2005):1031–1035, . DOI: https://doi.org/10.1016/j.electacta.2005.05.041.

[46] M. Hronec and J. Cvengrosova, Z. andKizlink. *J. Mol. Catal.*, **83**(1993):75–82. DOI: https://doi.org/10.1016/0304-5102(93)87008-V.

[47] P. K. Shen and C. Xu. *Electrochem. Commun.*, **8**(2006):184–188. DOI: https://doi.org/10.1016/j.elecom.2005.11.013.

[48] L. Zhao, O. Akdim, X. Huang, K. Wang, M. Douthwaite, S. Pattisson, R. J. Lewis, R. Lin, B. Yao, D. J. Morgan, G. Shaw, Q. He, D. Bethell, S. McIntosh, C. J. Kiely, and G. J. Hutchings. *ACS Catal.*, **13**(2023):2892–2903, . DOI: https://doi.org/10.1021/acscatal.2c06284.

[49] L. Vanoye, B. Guicheret, C. Rivera-Carcamo, J. Audevard, J. Navarro-Ruiz, I. del Rosal, I. C. Gerber, C. H. Campos, B. F. Machado, J. Volkman, R. Philippe, P. Serp, and A. Favre-Reguillon. *J. Catal.*, **424**(2023)(8):173–18. DOI: https://doi.org/10.1016/j.jcat.2023.05.006.

[50] N. Dimitratos, A. Villa, D. Wang, F. Porta, D. Su, and L. Prati. *J. Catal.*, **244**(2006):113–121, . DOI: https://doi.org/10.1016/j.jcat.2006.08.019.

[51] A. Villa, N. Janjic, P. Spontoni, D. Wang, D. S. Su, and L. Prati. *Appl. Catal., A*, **364**(009):221–228. DOI: https://doi.org/10.1016/j.apcata.2009.05.059.

[52] N. Dimitratos, J. A. Lopez-Sanchez, D. Morgan, A. F. Carley, R. Tiruvalam, C. J. Kiely, D. Bethell, and G. J. Hutchings. *PCCP*, **11**(2009):5142–5153, . DOI: https://doi.org/10.1039/B900151B.

[53] H. Keypour, J. Kouhdareh, R. Karimi-Nami, S. Alavinia, I. Karakaya, S. Babaei, and A. Maryamabadi. *New J. Chem.*, **47**(2023):6730–6738. DOI: https://doi.org/10.1039/D3NJ00307H.

[54] A. Ramazani, F. Sadri, A. Massoudi, M. Khoobi, S. W. Joo, L. Dolatyari, and N. Dayyani. **5**(2015):285–291, . DOI: https://doi.org/Iran. J. Catal.

[55] H. Aliyan, R. Fazaeli, A. R. Massah, H. J. Naghash, and S. Moradi. *Iran. J. Catal.*, **1**(2011):19–23.

[56] A. Ramazani, S. Taghavi Fardood, Z. Hosseinzadeh, F. Sadri, and S. W. Joo. *Iran. J. Catal.*, **7**(2017):181–185, .

[57] S. Iranfar, H. Ziyadi, M. Hekmati, E. Ghasemi, D. Esmaeili, and P. Haghighi. **11**(2021):347–354. DOI: https://doi.org/Iran. J. Catal.

[58] M. Tayebani, B. Shafaat, and M. Iravani. *Iran. J. Catal.*, **5**(2015):213–221.

[59] O. Clement, B. M. Rapko, and B. P. Hay. *Coord. Chem. Rev.*, **170**(1998):203–243. DOI: https://doi.org/10.1016/S0010-8545(98)00066-6.

[60] R. L. Chapman and R. S. Vagg. *Inorg. Chim. Acta*, **33**(1979):227–234. DOI: https://doi.org/10.1016/S0020-1693(00)89480-3.

[61] H. Sigel and R. B. Martin. *Chem. Rev.*, **82**(1982): 385–426. DOI: https://doi.org/10.1021/cr00050a003.

[62] P. C. A. Bruijnincx and P. J. Sadler. *Curr. Opin. Chem. Biol.*, **12**(2008):197–206. DOI: https://doi.org/10.1016/j.cbpa.2007.11.013.

[63] I. Ott and R. Gust. *Arch. Pharm.*, **340**(2007):117–126. DOI: https://doi.org/10.1002/ardp.200600151.

[64] M. J. Cleare. *Coord. Chem. Rev.*, **12**(1974):349–405. DOI: https://doi.org/10.1016/S0010-8545(00)82029-9.

[65] G. Angajala, V. Aruna, P. Pavan, and P. Guruprasad Reddy. *Bioorg. Chem.*, **119**(2022):105533. DOI: https://doi.org/10.1016/j.bioorg.2021.105533.

[66] M. Cortes-Clerget, N. Akporji, J. Zhou, F. Gao, P. Guo, M. Parmentier, F. Gallou, J. Y. Berthon, and B. H. Lipshutz. *Nature Communications*, **10**(2019):2169. DOI: https://doi.org/10.1038/s41467-019-09751-4.

[67] M. T. Mohammed, W. N. Al-Sieadi, and O. H. Al-jeilawi. *Eurasian Chemical Communications*, **4**(2022):481–494. DOI: https://doi.org/10.22034/ecc.2022.331659.1340.

[68] V. K. Bhovi, K. Bharathi, S. P. Melinmath, V. Basavanna, and S. Ningaiah. *Biointerface research in applied chemistry*, **12**(2021):3607–3617.

[69] V. S. Fedenko, S. A. Shemet, and M. Landi. *J. Plant Physiol.*, **212**(2017):13–28. DOI: https://doi.org/10.1016/j.jplph.2017.02.001.

[70] G. A. Gamov, M. N. Zavalishin, and V. A. Sharnin. *Spectrochimica Acta Part A: Molecular and Biomolecular Spectroscopy*, **206**(2019):160–164. DOI: https://doi.org/10.1016/j.saa.2018.08.009.

[71] G. Swiderski, A. Z. Wilczewska, R. Swislocka, M. Kalinowska, and W. Lewandowski. *J. Therm. Anal. Calorim.*, **134**(2018):513–525. DOI: https://doi.org/10.1007/s10973-018-7524-0.

[72] B. Gu, S. M. Cavaletto, D. R. Nascimento, M. Khalil, and S. Govind, N.and Mukamel. *Chem. Sci.*, **12**(2021):8088–8095. DOI: https://doi.org/10.1039/D1SC01774H.

[73] S. Boumendil, J. P. Cornard, M. Sekkal-Rahal, and A. Moncomble. *Chem. Phys. Lett.*, **636**(2015):39–45. DOI: https://doi.org/10.1016/j.cplett.2015.07.019.

[74] B. Zouchoune and L. Mansouri. *Struct. Chem.*, **30**(2019):691–701. DOI: https://doi.org/10.1007/s11224-018-1215-0.

[75] J. A. Peck, C. D. Tait, B. I. Swanson, and G. E. Brown. *Geochim. Cosmochim. Acta*, **55**(1991):671–676. DOI: https://doi.org/10.1016/0016-7037(91)90332-Y.

[76] G. Kalyuzhny, A. Vaskevich, G. Ashkenasy, A. Shanzer, and I. Rubinstein. *J. Physic. Chem. B*, **104**(2000):8238–8244. DOI: https://doi.org/10.1021/jp0010785.

[77] B. Karimi, M. Khorasani, H. Vali, C. Vargas, and R. Luque. *ACS Catal.*, **5**(2015):4189–4200. DOI: https://doi.org/10.1021/acscatal.5b00237.

[78] F. Li, Q. Zhang, and Y. Wang. *Appl. Catal., A*, **334**(2008):217–226, . DOI: https://doi.org/10.1016/j.apcata.2007.10.008.

[79] R. Bayan and N. Karak. *ACS Omega*, **2**(2017):8868–8876. DOI: https://doi.org/10.1021/acsomega.7b01504.

[80] M. M. Dell'Anna, M. Mali, P. Mastrorilli, P. Cotugno, and A. Monopoli. *J. Mol. Catal. A: Chem.*, **386**(2014):114–119. DOI: https://doi.org/10.1016/j.molcata.2014.02.001.

[81] X. Wang, G. Wu, N. Guan, and L. Li. *pplied Catalysis B: Environmental A*, **115-116**(2012):7–15, . DOI: https://doi.org/10.1016/j.apcatb.2011.12.011.

[82] G. J. Chen, J. S. Wang, F. Z. Jin, M. Y. Liu, C. W. Zhao, Y. A. Li, and Y. B. Dong. *Inorg. Chem.*, **55**(2016):3058–3064, . DOI: https://doi.org/10.1021/acs.inorgchem.5b02973.

[83] J. Wang, S. A. Kondrat, Y. Wang, G. L. Brett, C. Giles, J. K. Bartley, L. Lu, Q. Liu, C. J. Kiely, and G. J. Hutchings. *ACS Catal.*, **5**(2015):3575–3587, . DOI: https://doi.org/10.1021/acscatal.5b00480.

[84] Y. Li, J. Huang, X. Hu, W. Lam, F. L. Y. Wang, and R. Luque. *J. Mol. Catal. A: Chem.*, **425**(2016):61–67, . DOI: https://doi.org/10.1016/j.molcata.2016.09.030.

[85] S. Ghorbani, R. Parnian, and E. Soleimani. *J. Organomet. Chem.*, **952**(2021):122025. DOI: https://doi.org/10.1016/j.jorganchem.2021.122025.